The 2014 World Congress on
Advances in Civil, Environmental, and Materials Research (ACEM14)
Busan, Korea, August 24-28, 2014

Local cracking stability analysis of super high arch dam

*Peng Lin[1)] , Qingbin Li, Dong Zheng, Senying Hu

State Key Laboratory of Hydroscience and Engineering, Tsinghua University, Beijing 100084, China

[1)] celinpe@tsinghua.edu.cn

ABSTRACT

A local cracking problem of the Xiluodu super-high dam is first introduced and also the related horizontal cracking propagation risk during the construction and the operational period. Using a 3D FEM to analyze the cracking risk to the dam of a real crack at elevation 358.8~361.8 m, the results show that: 1) under normal water loading the state of the dam including stresses, deformations and the safety factor is very little affected; 2) after overloading to four times normal water pressure, at around 360m above the dam base, crack propagation, crack coalescence and yield damage would occur; 3) if the cracks are not reinforced, the dam overall stability is affected, reducing the bearing capacity and limiting the safety factor. Site deformation monitoring shows that current compression deformation is -0.02mm, and the proportion of that value due to the cracking is -0.01mm. The numerical predictions on cracking stability correlate well with field monitoring evidence.

1. INTRODUCTION

Although arch dams show good overload capability and a good safety record, dam structures have always been troubled by the cracking issue (Ingraffea 1990, Lin 2011, Lin 2014). The arch dam cracking phenomenon is almost as old as the history of the arch dam itself. As early as 1898, the Tammwarth arch dam (Zhang 2003) cracked because of the drought heat in summer and contraction due to cold in winter. Currently, the Chinese super high arch dams have also encountered cracking problems during construction and during operation. For example, part through cracks were found inside the Xiaowan arch dam (Lin 2014).

Xiluodu arch dam is an under construction super high arch dam situated on the Jinshajiang River in Yongshan County, Yunnan Province, southwest China. The dam is a concrete double curvature arch with a maximum height of 285.5 m. Two cracks were found on the upstream surface of the 20# transverse joints on May 22, 2010, illustrated in Fig.1. The crack elevations were at 358.8 and 361.8 m, with lengths of 1.3, 4.56 meters, respectively, and a maximum width of 0.08 mm. Seepage would take place along the crack propagation direction. A water pressure test showed that the crack

plane distribution was segmented and discontinuous. The crack 1# of the 20# dam section was located in the upstream side of the deck surface (Fig. 1(a)), with a length of 9.74m, and a maximum width of 0.12 mm.

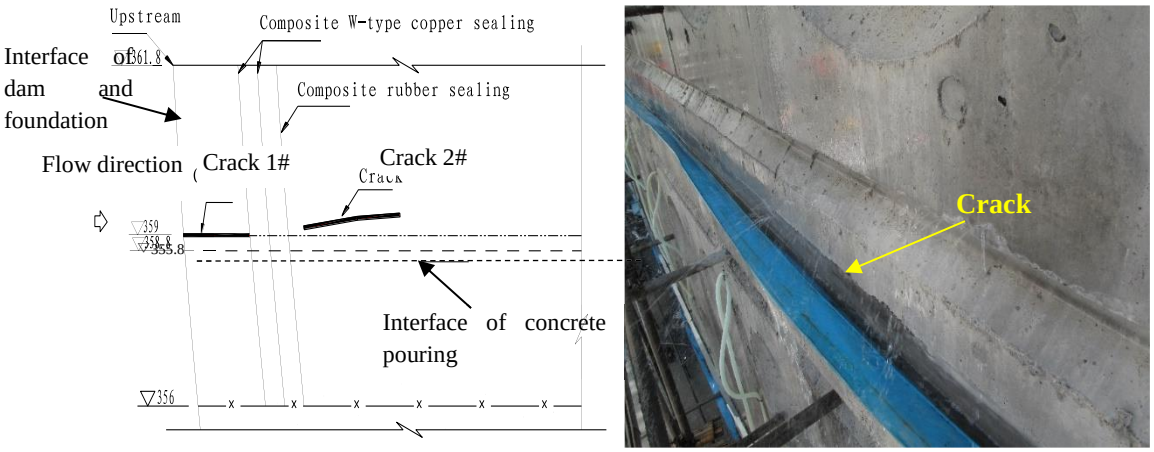

(a) Cross section map (b) Snapshot of dam cracking position

Fig.1 The range of horizontal cracks of 20# monolith at EL 358.8~361.8 m

Figure 1 shows the cracking states at elevation level (EL) 358.8~361.8 m above the upstream surface. If tension stress develops close to cracks, the inability of unreinforced concrete to carry tension may permit the formation of new cracking. Tension stress zones are almost certain to develop in a cracked dam and crack growth is apt to occur on the upstream surface at the junction of the dam and foundation. If water infiltrates the crack, and causes hydraulic fracturing, the cracks propagate and coalesce which has a serious effect on dam structural function and dam safety. Thus, a preliminary analysis based on the assumption that the concrete and rock material is capable of carrying some tension is usually necessary in order to discover the approximate location of the tension areas.

In this paper, crack influence on Xiluodu arch dam overall working state derived using numerical simulation and the crack propagation and crack stability mechanism were all analyzed and explored.

2. ANALYSIS METHODOLOGY AND MODEL

2.1 Mesh model

For the Xiluodu project site, a 3D finite element model was constructed as in Fig. 2(a). The represented size of the 3D numerical model was 1,000×1,500×661 m (length×width×height). As shown in Fig. 2(a), the 3D numerical model is extended at least as much as the dam height in the upstream direction, i.e. 300 m, about twice the dam height to each side i.e. 750 m, and twice the dam height in the downstream

direction, i.e. 700 m. All the rock masses together with their geological structures inside those ranges were represented in the 3D numerical model. The rock masses surrounding the dam within those ranges are types II, III1, III2, IV1, IV2 and V rock masses and the major rock masses under the dam are types II, III1 and III2. The geological structures in the ranges include the inter-strata bedding planes C9, C8, C7, C3, C2 and C1 and the intra-strata rupture belts Lc6 and Lc5. The physical-mechanical properties of the rock masses, the geological structures (i.e. weak zones) and the arch dam are listed in Lin et al.(2014).

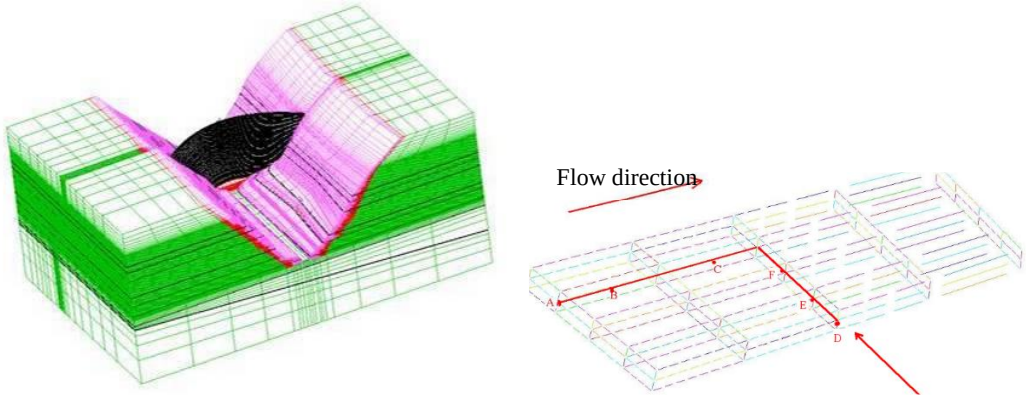

(a) 3D finite element mesh (b) Location of crack tip in dam body

Fig. 2 3D finite element and local model of the Xiluodu arch dam and its foundation

The cracks were located at EL 358.8m of No.20 dam monolith. To obtain boundary conditions for the cracking region, the larger, vertical direction range for the local crack model was assumed to be about 30m above 358.8 and about 15m below. The vertical distance is 15m from EL 358.8m to interface of dam-foundation. That is, the local model was taken as from EL 342.5m to EL 390.5m. Along the river direction, the cracking model stretched from the upstream face to the downstream face. In the transverse direction, the model stretched from the 19# transverse joints to the 20# transverse joints. In the local model, the crack faces tips were a set of single-nodes, but the nodes along the crack faces are dual nodes, which stretch from crack tip to crack end. The degenerate singularity elements and crack tip nodes are shown in Fig. 2(b).

During analysis, the node displacements of the overall model are applied to the local model as the boundary conditions, and the displacement constraints applied to the local model boundary nodes. The stability of the crack tip between points A and F could be judged by comparing calculated values of the stress intensity factor KI and the experimental value of fracture toughness KIc.

2.2 Analysis cases and properties of materials

ABAQUS (Hibbitt 2001) was employed to perform the finite element analysis and the elemental behavior follows the Drucker - Prager model (Cela 2002). In order to simulate crack evolution in a dam structure as the water load increases, and predict

crack growth and evaluate cracking risk to structural integrity, the analysis cases were divided between the construction(case 1) and operational periods (cases 2-5).

Case 1: Self-weight(dam pouring height EL601m) +upstream water loading(EL 540m) + downstream water load(EL378m) + temperature decrease

Case 2, and case 4 considered one and four times upstream normal water loading, respectively, and other loadings are the same Case1. The cases 3 and 4 considered water loading on crack surface based on Cases 2,and 4.

The self-weight of the dam and its abutments are the main loads in these analyses. According to the numerical results obtained from analysis cases No. 1 to No. 7, the local crack propagation mechanism and the effects on dam overall stability can be determined and discussed. The physical-mechanical properties of dam concrete and different rock mass types are referenced Lin et al.(2014).

3 CRACK STABILITY ANALYSIS

3.1 Analysis of crack stability during construction period

The deformed state of the local crack model during construction is illustrated in Fig. 3(a). It is shown that: the crack faces at EL 358.8m were in a closed state, because the weight loadings played an important role in effecting this. The crack stability during construction analysis results are listed in Table 1. It is shown that the crack tips at the points A, B and C were in a stable state during construction, and the cracks would not propagate in the transverse direction. Meanwhile, the crack tips at points D, E and F were in a stable state, and the cracks would not propagate in the river direction.

Table 1 Analysis of crack stability during construction and operating period

Working condition	Stress intensity factor of crack tip (MPa·m$^{1/2}$)	A point	B point	C point	D point	E point	F point
case 1	Ⅰ mode K_I	-11.59	-7.34	-3.68	-24.82	-18.97	-1.77
	Stability judging	Stable	Stable	Stable	Stable	Stable	Stable
Normal water level (case 2)	Ⅰ mode K_I	-59.75	-18.85	-17.46	-22.97	-11.57	-1.73
	Stability judging	Stable	Stable	Stable	Stable	Stable	Stable
Normal water level and fissure water (case 3)	Ⅰ mode KI	-30.56	-29.26	-13.10	25.71	24.26	22.64
	Stability judging	Stable	Stable	Stable	Instability	Instability	Instability
Four times normal water level	Ⅰ mode K_I	-147.71	-133.79	-105.10	55.49	97.44	117.88
	Stability judging	Stable	Stable	Stable	Instability	Instability	Instability
Four times normal water level and fissure water	Ⅰ mode K_I	-123.73	-119.40	-95.55	92.47	124.89	113.14
	Stability judging	Stable	Stable	Stable	Instability	Instability	Instability

** " negative" represents crack compression*

3.2 Analysis of crack stability during operating period

(1) Normal water loading

The deformed state of the local crack model under normal water loading is shown in Fig. 3(b). It is shown that the crack faces at elevation 358.8 m do not open and are in a closed state. However, comparing this situation with its state during construction, the closure of the crack faces is weakened, the crack tips of the faces are still in a state of compression.

transverse river direction river direction transverse river direction river direction

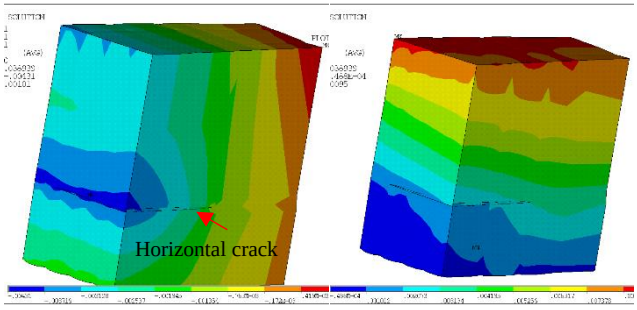

(a) During construction

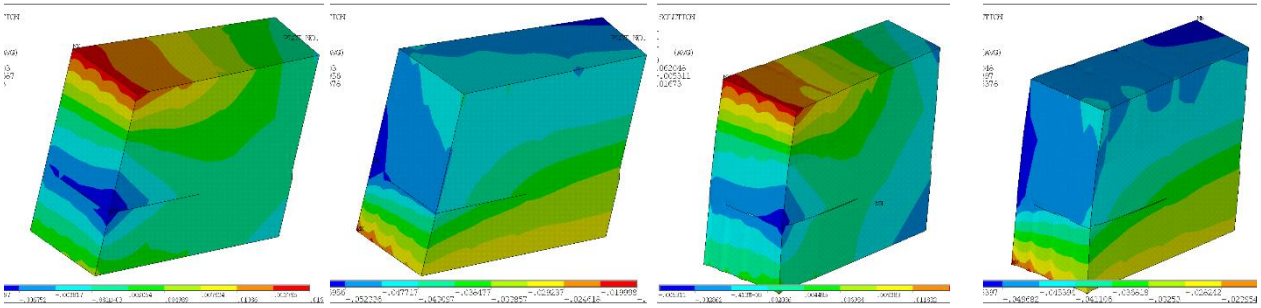

(b) Under normal water level （c）Under normal water level and fissure water

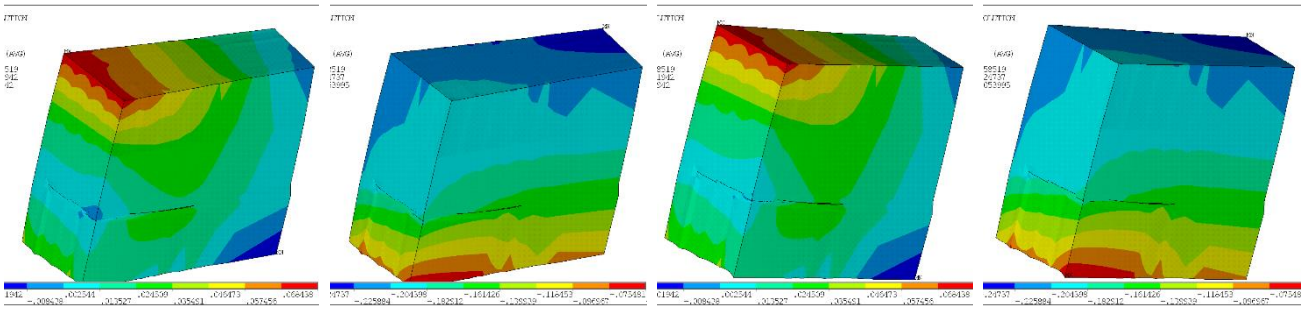

(d) Under four time normal water level (e) Under four time normal water level and fissure water

Fig.3 Deformed state of local crack model under different analysis cases

Considering the most unfavorable conditions, it is assumed that no water head loss

occurs along the crack faces, that is, the crack faces are exposed to a rectangular water head. The deformed state of local crack models under normal water level and fissure water pressure is shown in Fig. 3(c). It is shown that the crack faces at points A, B and C would not open and remain in the closed state. But the crack faces at D, E and F have already opened.

The crack stability analysis results representing the operating period are listed in Table 2. It is shown that: the crack tips at the points A, B and C are in a stable state under normal water level and also normal water level and fissure water, and that the cracks do not propagate in the transverse direction, perpendicular to the river. Meanwhile, the crack tips at points D, E and F are in a stable state under normal water level, and the cracks do not propagate in the river direction. The crack tips at points D, E and, F, however, are in a state of instability under normal water level and fissure water, and the cracks do propagate in the river direction.

(2) Overloading

The deformed state of the local crack model under four times the normal water loading is shown in Fig. 3(d). The deformed state of the local crack model under four times the normal water loading level and with fissure water loading is shown in Fig. 3(e).

Due to the weakening effect of the crack, the crack faces along the river are constantly in a state of compression, resulting in the crack faces in the perpendicular transverse direction changing gradually from a state of compression into the open state. The crack tips at the points A, B and C remain in a stable state under this overloading. The crack tips at points D, E and F, however, are in an unstable state under overloading, and the cracks will propagate in the river direction.

The crack stability analysis results under conditions of overloading (four time normal water level and four time normal water level and fissure water) are listed in Table 2. It is shown that: the crack tips at points A, B and C are in a stable state, and the cracks will not propagate in the transverse direction. Meanwhile, the crack tips at points D, E and F are in an unstable state and the cracks will propagate in the river direction.

3.3 Discussion of crack propagation

The existing cracks at the 20# monolith were all in a state of compression during construction and did not propagate. Those existing cracks remain in a state of compression under normal water loading during the operating period and the cracks will not propagate. Under normal water loading and fissure water loading, the existing cracks cannot propagate in the transverse direction, but there is high probability that they will propagate in the river direction.

Under four time normal water loading, the existing 20# monolith cracks will not propagate in the transverse direction, but will propagate in the river direction. Under four times the normal water loading and fissure water loading, there is a low probability of the existing cracks propagating in the transverse direction, but they will propagate in the river direction.

4 CONCLUSIONS

This paper describes the Xiluodu super-high dam being constructed in southwestern China as a case study, specifically to investigate horizontal cracking stability. The following conclusions can be drawn:

(1) The cracked zone at EL 358.8m was in a closed and compressive state under construction. If water enters the crack under normal water loading, the crack tips are stable in the transverse direction and perpendicular to the river flow direction. In the river flow direction, however, the crack tips propagate to the downstream surface of the dam.

(2) Under normal water loading, the crack has little effect on the transverse displacement. The crack in the 20# dam monolith, however, does influence dam overall displacement under conditions of overload. Based on yielded zone results, cracks at EL 358.8~361.8m, have little effect on the state of the dam including stresses, deformations and the safety factor under normal water loading. After overloading with four times normal water pressure, effects on the dam in the vicinity of EL 360m and in the dam base, were a proneness to crack propagation, coalescence and yield damage.

ACKNOWLEDGEMENTS

This research work was supported by National Natural Science Foundation of China (No: 11272178), National Basic Research Program of China (973 Program) Grant No. 2013CB035902, 2011CB013503, Tsinghua University Initiative Scientific Research Program.

REFERENCES

Cela, J.JL. (2002), “Material identification procedure for elastoplastic Drucker-Prager model”, *Journal Of Engineering Mechanics-asce*, 128(5):586-591

Hibbitt, K., Sorensen (2001), “ABAQUS/Standard user's manual”, Hibbitt, Karlsson & Sorensen.

Ingraffea A.R. (1990), “Case studies of simulation of fracture in concrete dams”, *Engineering Fracture Mechanics*, Vol. 35(1–3), 553-564

Lin P., Wang R.K., Kang S.Z., Zhang H.C., Zhou W.Y. (2011), “Study on key problems of foundation failure, reinforcement and stability for super high arch dams”, *Chinese Journal of Rock Mechanics and Engineering*, 30(10), 1945-1958

Lin P., Liu H.Y., Li Q.B., Hu H. (2014), “Effects of outlets on cracking risk and integral stability of super high arch dams”, *The Scientific World Journal*, Doi:10.1155/2014/312827

Lin P., Zhou W.Y., Liu H.Y. (2014), “Experimental study on cracking, reinforcement and overall stability of the Xiaowan super-high arch dam”, *Rock mechanics and rock engineering*, DOI: 10.1007/s00603-014-0593-x

Zhang D.Q., Chen H.B. (2003), “On design of Arch Dams based on analysis of cracks of some arch dam”, *Design of hydroelectric power station*, 19(3), 12-14